Synthesis and characterization of highly dispersed molybdenum carbides in mesoporous silica

Jean-Yves Piquemal[a], Claude Potvin[b], Jean-Marie Manoli[b,*], and Gérald Djéga-Mariadassou[b]

[a]*Laboratoire ITODYS –LCMDC, Université Denis Diderot, CNRS UMR 7086, Case 7090, 2 place Jussieu, 75251 Paris cedex 05, France*
[b]*Laboratoire de Réactivité de Surface, Université Pierre et Marie Curie, CNRS - UMR 7609, Case 178, 4 place Jussieu, 75252 Paris cedex 05, France*

Received 5 August 2003; accepted 25 November 2003

Highly dispersed molybdenum carbides in MCM-41 mesoporous silica are synthesized by temperature-programmed carburization and are characterized. Two methods of preparation are examined: (i) insertion of molybdenum during the synthesis of the MCM-41 silica and (ii) postsynthesis incorporation into a MCM-41 silica matrix by the incipient wetness method. Propene transformation (hydrogenation and metathesis) was used as a probe reaction; the observed catalytic behavior can be explained as a result of the preparation method, i.e., of the relative strength of interaction between the molybdenum oxide precursor and the support.

KEY WORDS: molybdenum; carbide; mesoporous; metathesis; propene.

1. Introduction

Since their discovery at the beginning of the 1990s [1–4], the new mesoporous materials of the MCM-41 type have received an increasing attention from many researchers working in various domains, such as material science [5], separation techniques and catalysis [6].

These materials are solids consisting of SiO_4 tetrahedra in which Al or another metal replaces some of the Si atoms. Shortly after the discovery of MCM-41, Corma *et al.* [7] used Al-MCM-41 to support Ni-Mo species in order to prepare catalysts for hydrocracking of a vacuum gas oil. The catalyst was investigated in terms of its activity in hydrodesulfurization (HDS) and denitrogenation (HDN). It is interesting to note that most research has focused on Al-MCM-41, probably in the hope that the acidity of the support will improve the activity; few papers have dealt purely with silica MCM-41 as a support for hydrotreating catalysts.

Molybdenum-impregnated (promoted with Ni or Co) MCM-41 was used to transform refractory compounds (dibenzothiophene, [8]). Catalysts consisting of molybdenum incorporated into MCM-41 mesoporous sieves have been little studied [9,10].

We recently reported an original approach for incorporating transition metal species into the mesostructured silica matrix on the basis of the use of low-nuclearity peroxidic species in an acidic medium (denoted the peroxo route) [11–13]. These catalysts present high metal incorporation levels (Si/M molar ratio down to 25; M = Mo, W), with a nearly homogeneous distribution of the dopants.

Molybdenum carbides and nitrides exhibit catalytic activities as high as those of the best noble metals [14]. For example, supported molybdenum carbide catalysts show activities in benzene hydrogenation comparable to those of Pt or Ru, whereas metallic molybdenum is much less active and stable than its carbide [15]. Although significant results have been obtained in the preparation of high surface area bulk materials [16,17], their synthesis is not straightforward because of the high temperatures involved. It is therefore very attractive to take advantage of high surface area supports such as alumina [18] and mesoporous silica.

In this paper, we present the synthesis and the characterization of molybdenum carbides on MCM-41 silica. Two molybdenum-containing material precursors are considered, differing in the metal incorporation mode: (i) direct insertion at the initial step of synthesis or (ii) impregnation of a pure silica MCM-41 support with an aqueous solution of the molybdenum precursor (ammonium heptamolybdate (AHM)). These materials were tested in propene hydrogenation.

2. Experimental

2.1. Materials

Tetraethyl orthosilicate (TEOS) (purum 99%), cetyltrimethylammonium chloride (CTMACl) (25 wt% in water) and MoO_3 (purum 99.5%) were purchased from Fluka. Aqueous H_2O_2 (30 wt%), AHM and

* To whom correspondence should be addressed.
E-mail: jmm@ccr.jussieu.fr

1011-372X/04/0200–0189/0 © 2004 Plenum Publishing Corporation

$(NH_4)_6[Mo_7O_{24}] \cdot 4H_2O$ were purchased from Prolabo and aqueous HCl (37 wt%) from Carlo Erba.

2.2. Catalyst preparation

The molybdenum-inserted mesoporous material, denoted by Mo-MCM-41, was prepared using low-nuclearity molybdenum peroxo complexes [11,12] with a starting Si/Mo molar ratio equal to 40, following the counter-ion-mediated $S^+X^-I^+$ pathway in a highly acidic medium [19]. MoO_3 (0.45 g, 3.125 mmol) was first treated with 15 wt% aqueous H_2O_2 (6 mL, 29.5 mmol). After 1 h of stirring at 60 °C, the solution, denoted by A1, was cooled to room temperature (RT). TEOS (28 mL, 0.125 mol) was mixed with a solution of CTMACl (20 mL, 15 mmol) and 12.5 M HCl (92 mL, 1.15 mol) in H_2O (220 mL, 17 mol); solution A1 was then quickly added. The composition of the gel was 1 TEOS/0. 12 CTMACl/8.9 HCl/137 H_2O/0.23 H_2O_2/0.025 MoO_3. The reaction mixture was stirred (200 rpm) at RT for 1 h. A pale yellow solid was isolated by filtration, washed with distilled water and dried over P_4O_{10} to give the native sample. A porous solid was obtained by calcination in air (150 cm^3 min^{-1}) from RT to 923 K (heating rate: 1 K min^{-1}, 4 h at the final temperature). The Si/Mo ratio of the product obtained was about 25 (table 1). The introduction of Mo into MCM-41 became difficult with decreasing Si/Mo in the gel: no mesostructured Mo-MCM-41 material was obtained with an initial Si/Mo = 20, and after calcination, MoO_3 was detected in the XRD pattern.

An all-silica MCM-41 was also prepared following the counter-ion-mediated $S^+X^-I^+$ pathway in a highly acidic medium, according to the method described previously [19]. Template-free material was obtained as described above.

The molybdenum-based catalyst supported on MCM-41 silica, denoted by Mo/MCM-41, was prepared by the incipient wetness method (capillary impregnation). Two grams of the predried MCM-41 support (at 353 K for 24 h) were impregnated with an aqueous solution of AHM at the required concentration. The resulting gel was then left at RT for 24 h and dried at 353 K for 24 h before calcination in air (150 cm^3 min^{-1}) from ambient to 773 K (heating rate: 1 K min^{-1}, 2 h at the final temperature).

Inserted and supported molybdenum carbide, denoted by MoC-MCM-41 and MoC/MCM-41 respectively, were prepared by temperature-programmed carburization (TPC). Carbide synthesis was divided into two steps. First, the samples were heated in argon (flow rate: 40 cm^3 min^{-1}) from RT to 718 K (heating rate: 1 K min^{-1}), the material was then carburized by TPC in flowing CH_4/H_2 (30% v/v mixture, total flow rate: 83.3 cm^3 min^{-1}), the temperature being raised linearly from 673 to the desired temperature (973, 1003, 1033, 1063 or 1093 K). At this final temperature, the CH_4/H_2 flow was switched to hydrogen and the material was cooled to RT for 1 h. After cooling, the supported carbides were passivated with 1% O_2/Ar (v/v) at RT for about 1 h before characterization and catalytic runs.

2.3. Characterization

Chemical analyses were carried out for calcined products before carburization at the Service Central d'Analyse (CNRS-Lyon) by inductive coupling plasma-atomic emission spectroscopy (ICP-AES) after alkaline fusion with $Li_2B_4O_7$.

X-Ray diffraction patterns (Cu Kα radiation) were obtained on a Siemens D500 diffractometer. The data were recorded with a 0.02 step-size, 8 s at each step-time in the range $2^\circ < 2\theta < 100^\circ$. The measurements were analyzed using EVA software developed by SOCABIM, France.

Adsorption and desorption isotherms for nitrogen were obtained at 77 K using a Micromeritics ASAP 2010. The samples were outgassed at 393 K and 0.1 Pa for 12 h before measurements were taken. Specific surface area (S_{BET}) values were obtained using the Brunauer-Emmett-Teller (BET) equation [20]; the mean

Table 1
Physicochemical characteristics of the mesostructures

Sample	Mo incorporation mode[a]	Treatment	$(Si/Mo)_{exp}$	Mo amount (wt%)	d_{100} spacing (Å)	Unit cell parameter (Å)	S_{BET} (m^2 g^{-1})	V_P (cm^3 g^{-1})	d_P[b] (Å)
MCM-41	–	–	∞	0	33	38	1235	0.66	21.4
Mo-MCM-41	I	–	23	7.1	32	37	1178	0.62	21.1
MoC-MCM-41	I	Carburization[c]	23	7.1	31	36	1268	0.66	20.8
Mo/MCM-41	IWM	Impregnation and drying	25	6.5	28	32	654	0.33	20.2
MoC/MCM-41	IWM	Calcination and carburization[c]	25	6.5	28	32	636	0.32	20.1

[a]I: incorporation into the gel; IWM: incipient wetness method.
[b]Average pore diameter $d_p = 4V_p/S_{BET}$.
[c]Carburization at 1003 K.

pore-size distributions were those of the Barrett-Joyner-Halenda (BJH) method [21], with the desorption branch being analyzed. Although the BJH method is usually considered to underestimate the real pore size [22], it can nevertheless be used for a qualitative estimation of the pore-size distribution. The mean pore diameters were calculated using the simple relation $4V_p/S_{BET}$, with V_p as the total pore volume.

TEM experiments were performed using a Jeol JEM 100 CXII transmission electron microscope operating at 100 kV. The samples were examined as thinly (70 nm) ultramicrotomed sections.

Raman spectra were recorded at RT with a Jobin Yvon U1000 spectrometer (excitation line, 514.5 nm of an Ar^+ ion laser; source power, 30–50 mW; resolution, 4 cm^{-1}). Solid samples are mounted on a rotating disk to avoid their decomposition and/or photoreduction under the laser beam.

Following Burwell *et al.* [23],, propene hydrogenation (a structure-insensitive reaction) was used as a model reaction to determine the properties of the materials at atmospheric pressure. The reaction was carried out in a flow reactor at 423 K. The gas mixture (the H_2/C_3H_6 molar ratio was fixed at 6.7 and the total flow rate at 12 cm^3 min^{-1}) was fed into a Pyrex reactor loaded with 0.1 g of catalyst on a sintered glass disk (diameter 1 cm). Catalytic results have to be interpreted cautiously, since we have not shown that the reaction of propene is not mass-transfer controlled. Nevertheless, the catalytic behaviors have been studied at the same reaction conditions and comparative studies are worthwhile. Moreover, note that the aim of this paper was not to evaluate absolute catalytic performances, but to discriminate between the two preparation methods through the nature of the reaction. The samples were pretreated as described above. The products of reaction (scheme 1) were separated and identified with a Hewlett–Packard 5890 series II gas chromatograph, equipped with a KCl-modified Al_2O_3 capillary column and a flame ionization detector. Steady state conversion was obtained after 6 h onstream and defined as the total amount of propene converted. Hydrogenation selectivity was calculated as

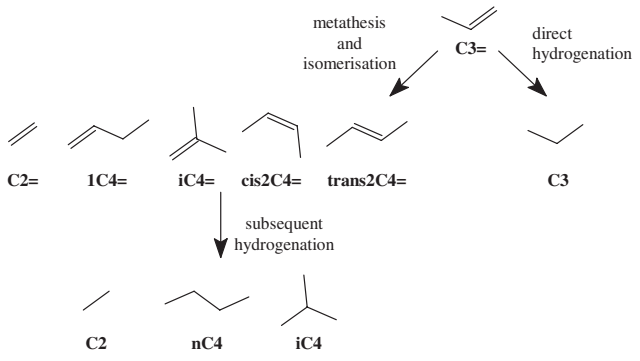

Scheme 1. Reaction products of propene hydrogenation and metathesis.

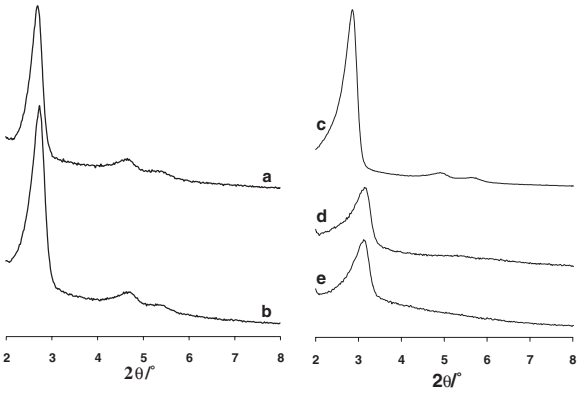

Figure 1. X-ray diffraction patterns of (a) calcined Mo-MCM-41; (b) Mo-MCM-41 carburized at 1003 K; (c) calcined MCM-41 silica; (d) dried MCM-41 silica after impregnation with an aqueous solution of AHM; (e) followed by calcination and subsequent carburization at 1003 K.

the amount of propene transformed directly to propane, and metathesis conversion as the amount of propene converted to C2 and C4 olefins, taking also into account the hydrogenated species (see scheme 1).

3. Results and discussion

3.1. Catalyst characterization

Powder X-ray diffraction patterns of the parent oxomolybdenum-inserted MCM-41 material and of that carburized at 1003 K (figure 1(a) and (b)) show three peaks that are assigned to the (100) (major strong reflection), (110) and (200) reflections of a hexagonal structure. The d_{100} values and unit cell parameters are listed in table 1.

Contrary to the MCM-41 silica support (figure 1(c)), the X-ray diffraction diagram (figure 1(d)) of the impregnated and dried material (but without subsequent thermal treatment) and of the carburized solid (figure 1(e)) show only one broad peak at low angle. Although Marler *et al.* [24] have shown that the intensities of the observed X-ray diffraction peaks are related to the difference in scattering power between the amorphous silicate wall and the in-pore amorphous organic phase, only for pure silica material and for molybdenum-inserted samples (Mo-MCM-41) higher order reflections, such as (110) and (200), are clearly visible.

Difference spectra calculated after intensity normalization for carburized (MoC-MCM-41), and calcined (Mo-MCM-41) materials show broad but distinct diffraction peaks at 2θ values of about 35–45° and 60–75° (figure 2). These diffraction peaks, specific of molybdenum carbide, cannot be indexed in the hexagonal system (β-Mo_2C, JCPDS 35-727) but in the cubic face-centered system (JCPDS 15-457) in agreement with the α-MoC_{1-x} molybdenum carbide reported by Bouchy *et al.* [25]. These results indicate that the inserted molybdenum species are transformed by carburization

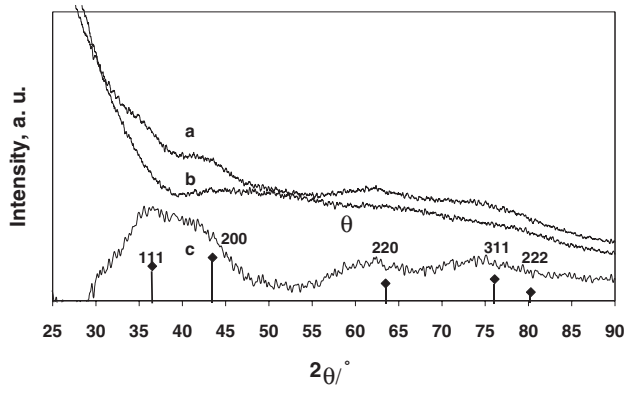

Figure 2. Difference X-ray diffraction pattern (c) between carburized MoC-MCM-41 (a) and calcined Mo-MCM-41 (b).

(CH_4/H_2) at 1003 K into α-MoC_{1-x}. A similar conclusion was noted in the literature [26] for the carburization of MoO_3/HZSM-5 by C_4H_{10}/H_2. The calculated unit cell parameter of the cubic face-centered structure was 0.435 nm. This value can be compared with that of 0.428 nm previously observed by Bouchy *et al*. [25] for α-MoC_{1-x} with an estimated stoichiometry of $MoC_{0.7}$. In contrast, no molybdenum carbide phase was detected in the difference spectra for MoC/MCM-41 and Mo/MCM-41. At first sight, this result is surprising. However, note that even if there is not a perfect distribution of the molybdenum centers, as is found in microporous TS-1, the "quasiperiodical" distribution of the molybdenum species in the silica matrix of Mo-MCM-41 may be responsible for the better crystallographic response.

The MCM-41 silica and the Mo-MCM-41 samples, before and after carburization, exhibit a reversible hysteresis-free type IV isotherm (see figure 3(a)). The surface areas, pore volumes and average pore diameters are in the same range for these three solids (see table 1), indicating that the Mo-MCM-41 has not been degraded during the carburization. In contrast, the specific surface area and the pore volume are significantly reduced (table 1) after the impregnation step with the aqueous AHM solution. On the other hand, the textural properties of the impregnated sample and of the subsequently carburized catalyst are nearly the same (see table 1), which can be interpreted by considering that the impregnation step is responsible for the partial degradation of the silica mesostructure. Note that, for highly siliceous Al-MCM-41, Cheng *et al*. observed a disastrous collapse of the mesoporous structure caused by the impregnation of aqueous AHM [27].

Raman spectroscopy is a useful technique for the characterization of metal oxide species incorporated into mesoporous materials [12,13,28–30]. Peaks at 246, 285, 292, 339, 668, and the two sharp absorptions at 820 and 995 cm^{-1} are due to bulk MoO_3 (figure 4(c)) [31,32] and can be seen in the spectrum of Mo/MCM-41 (see figure 4(b)), with the bands that originate from the SiO_2 matrix (380, 490 and a shoulder near 980 cm^{-1}). Two other vibrations at about 885 and 955 cm^{-1} are attributed to the Mo–O symmetric stretching mode and to the antisymmetric Mo–O–Mo stretch respectively [31].

Besides the bands of the mesoporous silica (223, 386, 501, 614 and 710 cm^{-1}), the Raman spectrum of Mo-MCM-41 (figure 4(a)) also shows these two stretches and, since no MoO_3 phase can be detected, these results show that direct incorporation of molybdenum, via the peroxo pathway, leads to a higher dispersion than that obtained by the impregnation.

Figure 5 shows HRTEM micrography of the MoC-MCM-41 sample taken at high magnification. The images reveal regular periodicity over very large areas

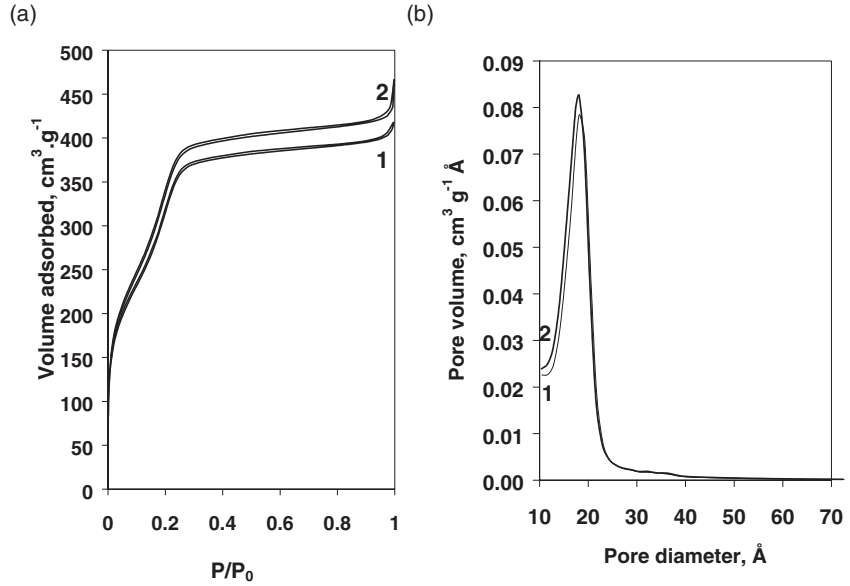

Figure 3. (a) N_2 adsorption–desorption isotherms of molybdenum-inserted samples: Mo-MCM-41 (1) and Mo-MCM-41 carburized at 1003 K (2), (b) pore-size distributions obtained by the BJH method, the desorption branch being analyzed.

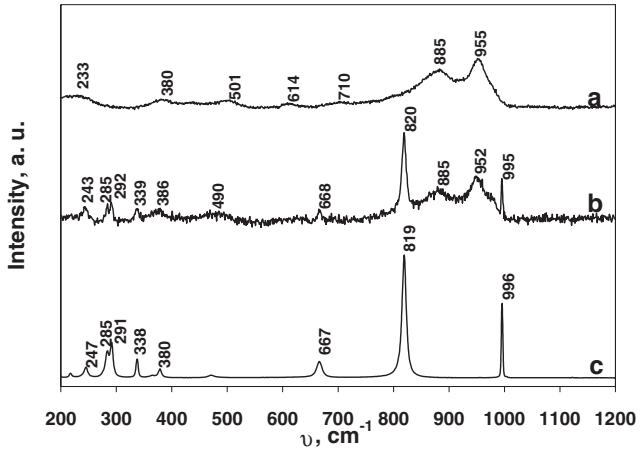

Figure 4. Raman spectra of the oxide precursors: (a) Mo-MCM-41, (b) Mo/MCM-41 and (c) bulk MoO_3.

and clearly indicate highly dispersed particles occluded within the nanotubes. We cannot exclude the presence of molybdenum carbide nanoparticles on the external surface of the material, although the ratio between external and internal surfaces is very low (in this work, less than 1%).

3.2. Propene reaction

With the two sets of catalysts, i.e., MoC-MCM-41 and MoC/MCM-41, hydrogenation as well as metathesis products was observed, in proportions depending on the molybdenum incorporation mode (insertion during synthesis or impregnation) and on the carburization temperature.

Analysis of the butenes formed revealed that 2-butene (cis and trans), 1-butene and isobutene are present. For all catalysts, the ethene/butene ratio is about 1, but the butene distribution is obviously perturbed by subsequent hydrogenation. The MoC/MCM-41 catalysts give higher propene conversion with a more pronounced hydrogenation selectivity.

Figure 6 shows the variation of the total conversion of propene, and of the hydrogenation and metathesis selectivities with the carburization temperature of MoC-MCM-41. The results clearly show that increasing carburization temperatures lead to a catalyst with higher hydrogenation activity, usually displayed by classical molybdenum carbides. For comparison, a Mo-MCM-41 material was reduced at 1093 K with hydrogen; molybdenum carbide is not formed, hence the catalytic activity (hydrogenation) is nearly inexistent (table 2).

Although the metathesis mechanism, proceeding through the initial formation of a carbene, which further reacts with another olefin to form a metallacycle [33], is well known and accepted, extremely divergent conclusions have been drawn concerning the oxidation state of the active metal species, with values in the range 0 to +VI [34]. On the other hand, *ab initio* mechanistic studies suggest that the oxygen ligand on high-valent Mo complexes is involved in the catalytic process [35].

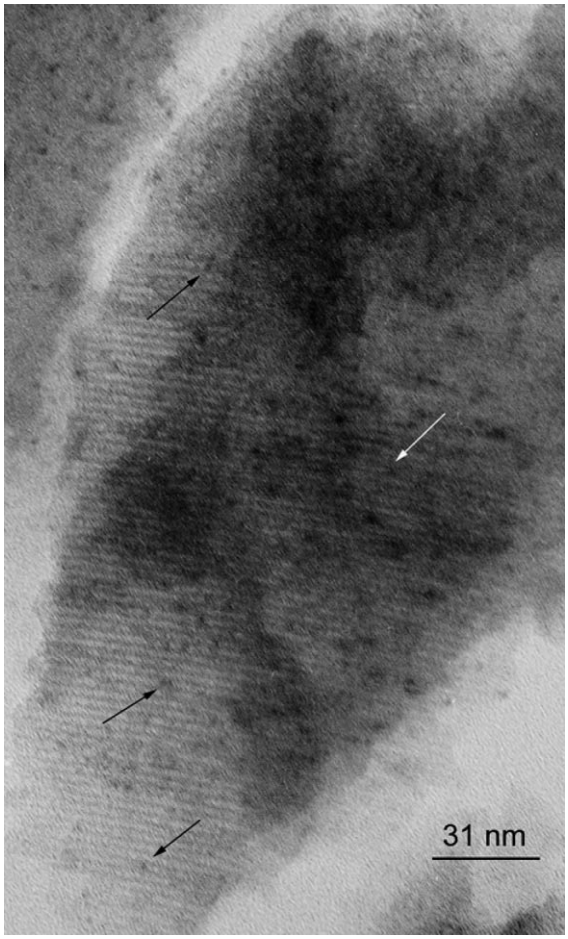

Figure 5. HRTEM micrography of MoC-MCM-41 showing molybdenum carbide particles.

As observed by Raman spectroscopy Mo–O bonds are still present at 1003 K (carburization temperature) in MoC-MCM-41. The carburization is not fully complete and a higher temperature is necessary to ensure total carburization (as shown by the higher hydrogenation

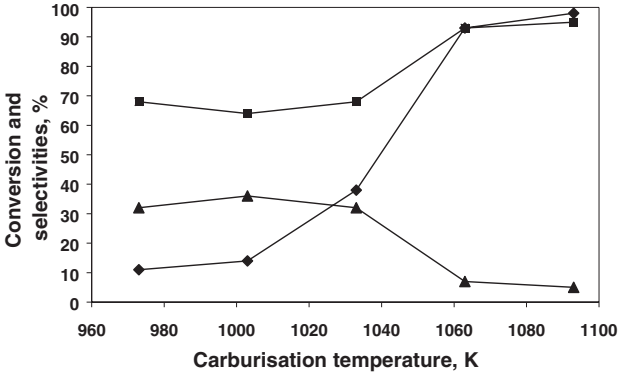

Figure 6. Effect of the reaction temperature of MoC-MCM-41 on the steady state conversion and selectivities. ▲ : metathesis selectivity; ■ : hydrogenation selectivity; ◆ : conversion.

Table 2
Propene hydrogenation at 423 K catalyzed by molybdenum-incorporated samples

					Reaction products (%)[c]							
					C2		C3	C4				
Sample	T_C[a] (K)	C[b] (%)	S_M[b] (%)	S_H[b] (%)	C2	C2=	C3	*n*C4	2C4=trans	2C4=cis	1C4=iso	C4=
MoC-MCM-41	1003	14	36	64	2.8	15.3	63.5	1.2	9.9	0.0	2.0	5.3
	1093	98	5	95	2.6	0.0	95.0	2.3	0.1	0.0	0.0	0.0
MoR-MCM-41[d]	–	2	0	100	0.0	0.0	100	0.0	0.0	0.0	0.0	0.0
MoC/MCM-41	1003	71	17	83	5.8	2.7	83.1	3.8	1.2	0.2	2.3	0.9

[a] T_C: temperature of carburization.
[b] C, S_M and S_H: total conversion, metathesis selectivity and hydrogenation selectivity respectively.
[c] Cx, paraffin; Cx=, olefin with x for the carbon atom number; trans, cis and iso: olefin isomers. The distribution of products is expressed in moles for 100 mol of product obtained in metathesis and hydrogenation.
[d] MoR-MCM-41: sample Mo-MCM-41 reduced at 1093 K under hydrogen.

selectivity, see table 2). The catalytic behavior of MoC/MCM-41 resembles more that of a classical supported molybdenum carbide. The interaction between the molybdenum carbide precursor and the silica support is weaker than that in the catalyst where molybdenum was incorporated during the synthesis.

4. Conclusion

Two sets of molybdenum-containing mesoporous silica catalysts have been synthesized and characterized by various physicochemical techniques. In the first procedure, molybdenum is introduced directly into the synthesis gel as peroxo complexes, while in the other procedure, molybdenum is incorporated in the mesopores of a template-free silica following the classical impregnation. The results clearly show that in the latter case, the impregnation step is responsible for a dramatic degradation of the mesoporous structure. On the contrary, with molybdenum-inserted solids, the mesostructure is preserved and the physicochemical data are in agreement with a high dispersion of the metal centres.

The catalysts have been tested in propene hydrogenation and the results obtained clearly differentiate the two catalysts. The different catalytic behavior is attributed to a stronger interaction of the molybdenum species with the silica matrix in the case of molybdenum-inserted mesostructured materials, leading to higher metathesis and reduced hydrogenation activities. In order to ensure total carburization of the molybdenum-inserted samples, a high temperature (1093 K) is required.

Acknowledgments

The authors gratefully thank Mrs. G. Chottard for the Raman experiments. Thanks are due to Prof. J.-M. Brégeault and Dr. J.S. Lomas for fruitful discussions and for correcting the manuscript.

References

[1] T. Yanagisawa, T. Shimizu, K. Kuroda and C. Kato, Bull. Chem. Soc. Jpn. 63 (1990) 988.
[2] T. Yanagisawa, T. Shimizu, K. Kuroda and C. Kato, Bull. Chem. Soc. Jpn. 63 (1990) 1535.
[3] C.T. Kresge, M.E. Leonowicz, J.W. Roth, J.C. Vartuli and J.S. Beck, Nature 359 (1992) 710.
[4] J.S. Beck, J.C. Vartuli, W.J. Roth, M.E. Leonowicz, C.T. Kresge, K.D. Schmitt, C.T.W. Chu, D.H. Olson, E.W. Sheppard, S.B. McCullen, J.B. Higgins and J.L. Schlenker, J. Am. Chem. Soc. 114 (1992) 10834.
[5] A. Stein, B.J. Melde and R.C. Schroden, Adv. Mater. 12 (2000) 1403.
[6] A. Sayari, Chem. Mater. 8 (1996) 1840.
[7] A. Corma, A. Martinez, V. Martinez-Soria and J.B. Monton, J. Catal. 153 (1995) 25.
[8] A. Wang, Y. Wang, T. Kabe, Y. Chen, A. Ishihara, W. Qian and P. Yao, J. Catal. 210 (2002) 319.
[9] D.-H. Cho, T.-S. Chan, S.-K. Ryu and Y.K. Lee, Catal. Lett. 64 (2000) 27.
[10] K.R. Rana and B. Viswanathan, Catal. Lett. 52 (1998) 25.
[11] J.-Y. Piquemal, J.-M. Manoli, P. Beaunier, A. Ensuque, P. Tougne, A.-P. Legrand and J.-M. Brégeault, Microporous Mesoporous Mater. 29 (1999) 291.
[12] J.-Y. Piquemal, E. Briot, M. Vennat, J.-M. Brégeault, G. Chottard and J.-M. Manoli, Chem. Commun. (1999) 1195.
[13] E. Briot, J.-Y. Piquemal, M. Vennat, J.-M. Brégeault, G. Chottard and J.-M. Manoli, J. Mater. Chem. 10 (2000) 953.
[14] S.T. Oyama, Catal. Today 2 (1992) 179.
[15] J.S. Lee, M.H. Yeom, K.Y. Park, I.S. Nam, J.S. Chung, Y.G. Kim and S.H. Moon, J. Catal. 128 (1991) 126.
[16] S.T. Oyama, J.C. Schlatter, J.E. Metcalfe and J.M. Lambert, Ind. Eng. Chem. Res. 27 (1988) 1639.
[17] L. Volpe and M. Boudart, Catal. Rev. Sci. 27 (1985) 515.
[18] P.D. Costa, C. Potvin, J.-M. Manoli, J.-L. Lemberton, G. Pérot and G. Dgéga-Mariadassou, J. Mol. Catal., A 184 (2002) 323.
[19] Q. Huo, D.I. Margolese, U. Ciesla, D.G. Demuth, P. Feng, T.E. Gier, P. Sieger, A. Firouzi, B.F. Chmelka, F. Schüth and G.D. Stucky, Chem. Mater. 6 (1994) 1176.
[20] S. Brunauer, P.H. Emmett and E. Teller, J. Am. Chem. Soc. 60 (1938) 309.
[21] E.P. Barrett, L.G. Joyner and P.P. Halenda, J. Am. Chem. Soc. 73 (1951) 373.
[22] M. Kruk, M. Jaroniec and A. Sayari, Microporous Mater. 9 (1997) 173.
[23] R.L. Burwell, Langmuir 2 (1986) 2.

[24] B. Marler, U. Oberhagemann, S. Vortmann and H. Gies, Microporous Mater. 6 (1996) 375.
[25] C. Bouchy, S.B.D.-A. Hamid and E.G. Derouane, Chem. Commun. (2000) 125.
[26] S. Yuan, S.B.D.-A. Hamid, Y. Li, P. Ying, Q. Xin, E.G. Derouane and C. Li, J. Mol. Catal., A 184 (2002) 257.
[27] M. Cheng, F. Kumata, T. Saito, T. Komatsu and T. Yashima, in *Studies in Surface Science and Catalysis*, L. Bonneviot, F. Béland, C. Danumah, S. Giasson and S. Kaliaguine (eds) (Elsevier, Amsterdam, 1998) p. 485.
[28] M.S. Morey, J.D. Bryan, S. Schwartz and G.D. Stucky, Chem. Mater. 12 (2000) 3435.
[29] L.-X. Dai, Y.-H. Teng, K. Tabata, E. Suzuki and T. Tatsumi, Microporous Mesoporous Mater. 44–45 (2001) 573.
[30] S. Che, Y. Sakamoto, H. Yoshitake, O. Terasaki and T. Tatsumi, J. Phys. Chem. 105 (2001) 10565.
[31] C.C. Williams, J.G. Ekerdt, J.-M. Jehng, F.D. Hardcastle, A.M. Turek and I.E. Wachs, J. Phys. Chem. 95 (1991) 8781.
[32] J.M. Stencel, *Raman Spectroscopy for Catalysis* (Van Nostrand Reinhold, New York, 1990).
[33] J.L. Hérisson and Y. Chauvin, Makromol. Chem. 141 (1970) 161.
[34] I. Rodriguez-Ramos, A. Guerrero-Ruiz, N. Homs, P. Ramírez de la Piscina and J.L.G. Fierro, J. Mol. Catal., A: Chem. 95 (1995) 147.
[35] A.K. Rappé and W.A.G. III, J. Am. Chem. Soc. 104 (1982) 448.